

# Computed tomography findings of COVID-19 in pediatric patients

Yeliz Dadalı<sup>1</sup>✉, Sercan Özkaçmaz<sup>2</sup>✉, Erdal Ünlü<sup>3</sup>✉, Rukiye Akyol<sup>4</sup>✉,  
Muhammed Alparslan<sup>1</sup>✉

Departments of <sup>1</sup>Radiology, <sup>3</sup>Child Health and Diseases and <sup>4</sup>Microbiology, Ahi Evran University Faculty of Medicine, Kırşehir;  
<sup>2</sup>Department of Radiology, Yüzüncü Yıl University Faculty of Medicine, Van, Turkey.

## ABSTRACT

**Background.** In this study, we aimed to evaluate the thorax Computed Tomography (CT) findings of pediatric patients diagnosed with coronavirus disease-19 (COVID-19) and to discuss these findings in light of the results of adult patients from the literature.

**Methods.** The CT scans of pediatric patients (1-18 years old) with a diagnosis of COVID-19 by reverse transcriptase-polymerase chain reaction (RT-PCR) in our hospital between March 2020 and January 2021 were retrospectively reviewed. The scans were interpreted regarding the distribution and localization features, and involvement patterns including ground-glass opacity, consolidation, halo/reversed halo sign, interlobular septal thickening, air bronchograms and bronchiectasis. The frequencies of these findings in pediatric cases in our study were recorded.

**Results.** A total of 95 patients with a mean age of 13±4.6 years were included in this study. Among them, 34 (36%) had lesions associated with COVID-19 on CT scans. Bilateral involvement was detected in 15 (44%) while unilateral in 19 (56%) patients. Eighteen (53%) patients had single lobe involvement. In 16 (47%) patients a solitary lesion was detected and in 18 (53%) multiple lesions were present. Ground-glass opacity appearance was observed in 28 (82%), consolidation in 9 (26%), and ground-glass opacity with consolidation in 8 (24%), halo sign in 9 (26%), reversed halo sign in 2 (6%), interlobular septal thickening (interstitial thickening) in 1 (3%) patients.

**Conclusions.** As symptoms are relatively milder in children with COVID-19, CT findings are less extensive than in adults. It is essential to know the thorax CT findings that aid in the diagnosis and follow-up of the disease.

**Key words:** COVID-19, children, computed tomography, chest imaging, pneumonia.

The number of pediatric COVID-19 patients is growing significantly. Although most children with COVID-19 have had mild clinical symptoms, cases with severe signs of disease or even death have been reported.<sup>1,2</sup> Early diagnosis of the infection in children is important, as they also increase the transmission risk. Thus, the Computed Tomography (CT) scans of children with a suspicion of pneumonia must be carefully

evaluated to both protect children and prevent spreading.<sup>1</sup>

The main diagnostic and screening tool for COVID-19 pneumonia is reverse transcriptase polymerase chain reaction (RT-PCR). However, the accuracy of the test depends on the quality of the throat swab and the viral load. Radiological features are very important for the diagnosis of COVID-19, and thorax CT can also detect pulmonary findings suggestive of COVID-19 infection even in patients who have initial negative RT-PCR results.<sup>3</sup>

While knowledge about the clinical and epidemiological features of COVID-19 in

✉ Sercan Özkaçmaz  
sercanozkacmaz@hotmail.com

Received 4th June 2021, revised 3rd March 2022,  
accepted 22nd May 2022.

children is rapidly increasing, large studies of radiological findings are still lacking. In this study, we aimed to present the radiological features of COVID-19 in children.

## Material and Methods

Thorax CT scans of pediatric patients who were admitted to our hospital between March 2020-January 2021 and diagnosed with COVID-19 by RT-PCR were retrospectively reviewed using the hospital database. CT examinations were performed with a 16-slice CT device (Toshiba Alexion 16) in a 3mm slice thickness in the supine position and the appropriate thoracic protocol (kVp: 100-120, mAs: 50-100). An intravenous or oral contrast agent was not administered to the patients. The images were sent to a workstation (Syngovia Siemens Medical System, Siemens/Germany) and evaluated in both the mediastinal and parenchymal windows in all three planes (axial, sagittal, and coronal). All the images were evaluated independently by two radiologists with 19 and 9 years of experience in thoracic imaging who were blinded to the each others interpretations. The final decisions were reached with consensus in cases of conflict.

The demographic characteristics of the patients including age, gender, and CT features of the lesions were examined. The location of the lesions was classified as unilateral-bilateral, anterior-posterior, central (parenchymal areas adjacent to the hilus)-peripheral (parenchymal areas close to the pleura) according to parenchymal involvement. The distribution of the lesions was classified as the right upper, middle, lower and left upper and lower lobe. The number of lobes affected was also examined. The morphological characteristics of the ground-glass opacities were classified as patchy or nodular forms. The morphological structure of the consolidation areas was described as round, linear or irregular. Interlobular septal thickening ("crazy paving"), tree-in-bud appearance, air bronchograms, bronchial wall thickening, bronchiectasis, air bubble, reversed halo sign, halo sign, nodule,

linear atelectasis, pleural thickening, pleural effusion, pericardial effusion, and mediastinal lymphadenopathy (lymph node short axis dimension >10mm) were identified as present or absent.<sup>4-6</sup>

Statistical analysis was performed using the SPSS program (IBM SPSS Statistics for Windows Version 21.0. Armonk, NY: IBM Corp, USA). The demographic variables were expressed as mean±standard deviation. Other variables were presented as number (N) and percentage (%). A Cohen's kappa coefficient ( $\kappa$ ) was calculated to assess the interobserver agreement between the two radiologists who interpreted the CT scans.

This study was approved by Kırşehir Ahi Evran University Ethics Committee on 09/02/2021 with the number of 2021-03 / 28.

## Results

A total of 95 pediatric patients were included in this study. Among them, 61 (64%) had no pathology on thorax CT. Of the 34 (36%) patients with positive CT findings, 19 (56%) were male and 15 (44%) were female. The mean age was 13 ± 4.6 (1-18) years. The interobserver agreement between the two radiologists was substantial ( $\kappa$ : 0.7925).

Bilateral involvement was detected in 15 (44%) patients. Among 19 (56%) patients with unilateral involvement, 10 (53%) had lesions on the right and 9 (47%) on the left lobe. Although the lower lobes were mostly affected, the upper lobes were also involved with a similar rate (Right upper lobe in 13 (38%), right middle lobe in 5 (15%), right lower lobe in 16 (47%), left upper lobe in 12 (35%), left lower lobe in 18 (53%) patients). Parenchymal lesions were present in one lobe in 18 (53%) patients, in two lobes in 8 (24%), in three lobes in 3 (9%), in four lobes in 3 (9%), and in five lobes in 2 (6%) patients (Table I).

Eighteen patients had single lobe involvement. Involvement rates were similar in all lobes except the right middle lobe (right upper lobe:

**Table I.** Distribution of lesions in lung areas.

Findings		N	(%)
Pathology	Absent	61	64
	Present	34	36
Affected lung side	Bilateral	15	44
	Unilateral	19	56
	Right	10	53
	Left	9	47
Affected lung lobe	Right upper lobe	13	38
	Right middle lobe	5	15
	Right lower lobe	16	47
	Left upper lobe	12	35
	Left lower lobe	18	53
Number of lobes affected	1	18	53
	2	8	24
	3	3	9
	4	3	9
	5	2	6
Single lobe involvement (n:18)*	Right upper lobe	4	22
	Right middle lobe	1	6
	Right lower lobe	4	22
	Left upper lobe	5	28
	Left lower lobe	4	22
Affected lung field	Anterior	4	12
	Posterior	26	76
	Anterior-Posterior	4	12
	Peripheral	29	85
	Central	0	0
	Both Central and Peripheral	5	15
Number of lesions	Single	16	47
	Multiple	18	53

\*Lobar distribution percentages in this heading referred the ratio of involvement number of each lobes to the patient number with single lobe involvement (n:18)

4 (22%), right middle lobe: 1 (6%), right lower lobe: 4 (22%), left upper lobe 5 (28%), left lower lobe: 4 (22%). In 26 (76%) patients, the lesions were located only in the posterior (posterior to the hilus), while 4 (12%) were located in the anterior (anterior to hilus) and 4 (12%) were both anterior and posterior parenchymal areas.

The lesions were located only in the peripheral regions of the lungs in 29 (85%) and both in the peripheral and in the central regions in 5 (15%) patients. There was no patient with only

a central lesion in this study. A single lesion was detected in 16 (47%) and multiple lesions in 18 (53%) patients.

Ground-glass opacity appearance was seen in 28 (82%), consolidation in 9 (26%), and ground-glass opacity with consolidation in 8 (24%) patients. These ground-glass opacities were nodular type in 15 (44%) patients, and patchy type in 8 (24%) patients (Fig. 1,2). In 5 (15%) patients, nodular and patchy ground-glass opacities were seen together (Table II).

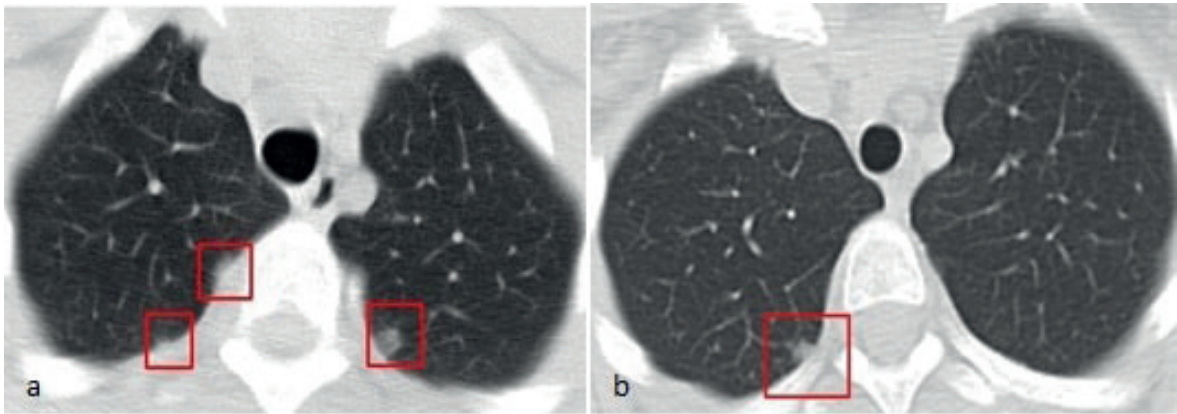


**Fig. 1a-b.** Peripheral nodular type ground-glass opacities in the bilateral upper lobes (a) in a 16 year old male (a) and a peripheral nodular type ground-glass opacity in a 17 year old male (b).



**Fig. 2.** A patchy peripheral ground-glass opacity in the right upper lobe in a 5 year old female.

Consolidation areas were only round-shape in 13 (38%), round+linear in 1 (3%), round+irregular in 2 (6%) and round+lineer+irregular in one patient (3%) (Fig. 3). All of the irregular and linear-shaped consolidation areas were accompanied by the round consolidation areas.

Nine (26%) patients had a halo (Fig. 4) and 2 (6%) had a reversed halo sign (Fig. 5). Seven (21%) patients had air bronchograms within areas of consolidation. Bronchiectasis was detected in 2 (6%) patients. Bronchial wall thickening was present in 3 (9%) patients (Fig. 6). Air bubble sign appearance was detected in 1 (3%) patient (Fig. 7). Vascular enlargement was present in 2 (6%) patients (Fig. 8). Interlobular septal thickening (interstitial thickening) was present in 1 (3%) patient (Fig. 9). Tree-in-bud appearance was detected in 3 (9%) patients (Fig. 10,11). Nine (26%) patients had subpleural and perivascular nodules with a mean diameter of  $4.6 \text{ mm} \pm 1.3$  (3-7 mm) (Fig. 12). Parenchymal band structure (atelectasis) was observed in 2 (6%) patients (Figure 13). Pericardial fluid was observed in 1 (3%) patient (Fig. 14). Lymphadenopathy and pleural fluid were not found in the patients.

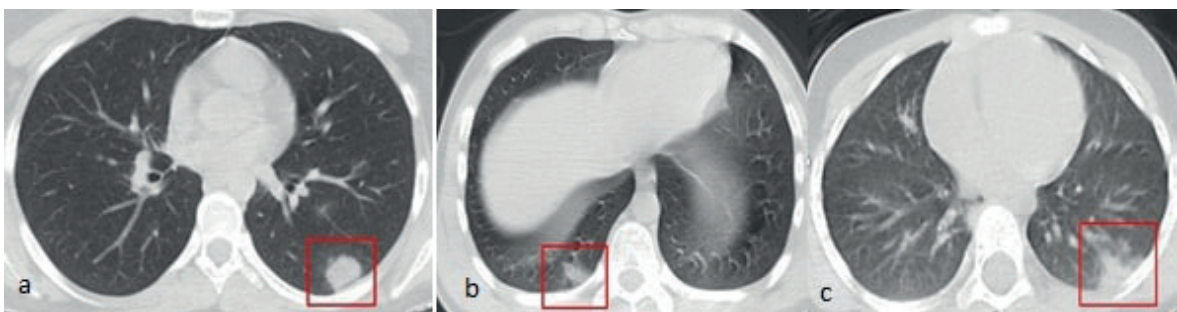


**Fig. 3a-c.** A peripheral round consolidation in the left lower lobe in a 15 year old female (a).A peripheral lineer consolidation in right lower lobe in a 15 year old male (b) and a peripheral irregular consolidation in the left lower lobe in a 5 year old female (c).

**Table II.** Frequency of parenchymal lesions.

Findings	N	%	
Ground-glass opacity	28	82	
Consolidation	9	26	
Ground-glass opacity with consolidation	8	24	
Ground-glass opacity morphology	Nodular	15	44
	Patchy	8	24
	Nodular + Patchy	5	15
	Round	17	50
Consolidation morphology (n:17)*	Linear	2	6
	Irregular	3	9
Air bronchogram	7	21	
Bronchiectasis	2	6	
Bronchial wall thickening	3	9	
Air bubble sign	1	3	
Vascular enlargement	2	6	
Interlobular septal thickening	1	3	
Halo sign	9	26	
Reversed halo sign	2	6	
Tree-in-bud sign	3	9	
Nodule	9	26	
Linear Atelectasis	2	6	
Pleural effusion	0	0	
Pericardial Effusion	1	3	
Lymphadenopathy	0	0	

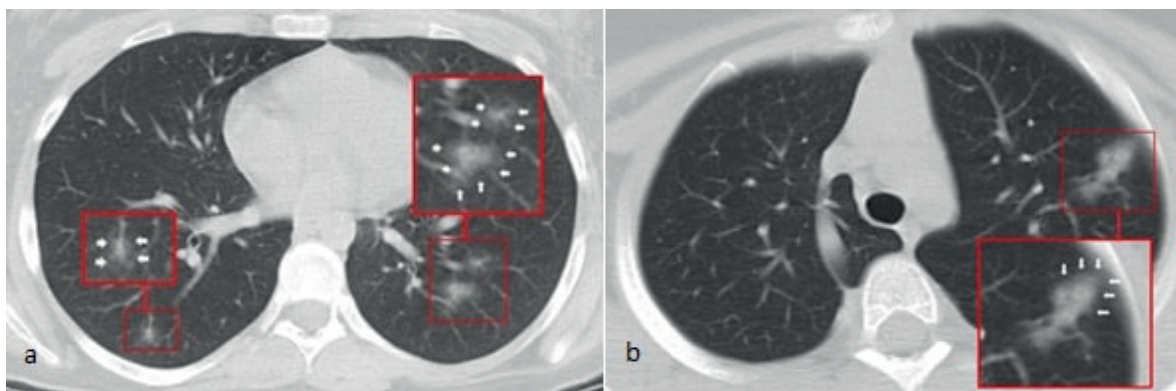


**Fig. 4a-b.** Multiple halo signs (white arrows) surrounding nodules in bilateral lungs in a 15 year old female (a) and in a halo sign (white arrows) surrounding nodules in the left upper lobe in a 14 year old female (b).

We identified 8 (24%) patients with multiple Ground-glass opacity appearances and multiple consolidation areas (Fig. 15). Among 3 patients with a control CT scan (7-15 days after the first scan) lesions completely resolved in 2 (Fig. 16)

while they remained in one patient, the lesions progressed and new lesions appeared (Fig. 17).

Among the 95 patients with CT scans, 42 had a prior chest X-ray. The X-rays were interpreted

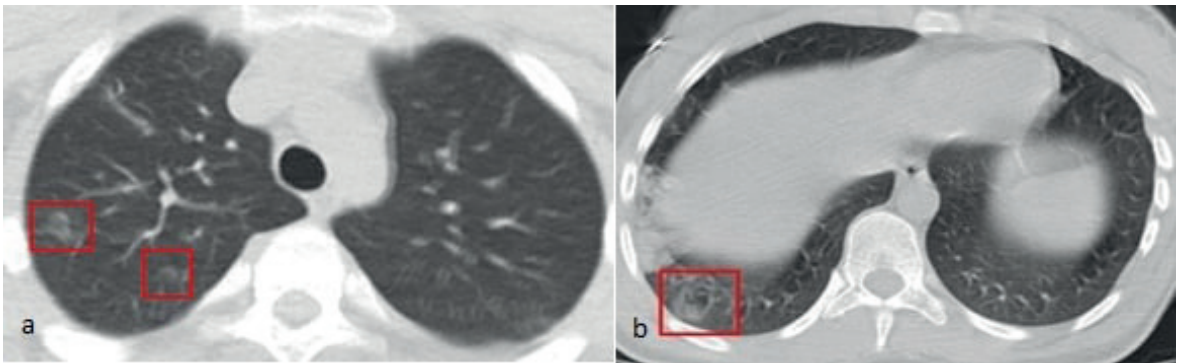


**Fig. 5a-b.** Reversed halo sign in right upper lobe in a 15 year old male (a) and in right the lower lobe in a 3 year old male (b).

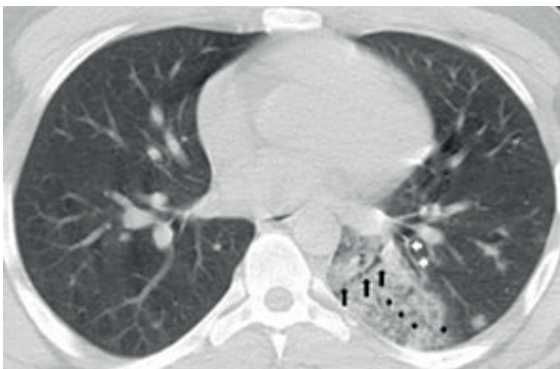


**Fig. 6.** Bronchiectasis (long black arrows), bronchial wall thickening (white arrows) and air bronchograms (short black arrows) within a central-peripheral consolidation in the left lower lobe in a 16 year old male.



**Fig. 8.** Vascular enlargement (white arrows) adjacent to a nodular consolidation in right lower lobe in a 17 year old female.

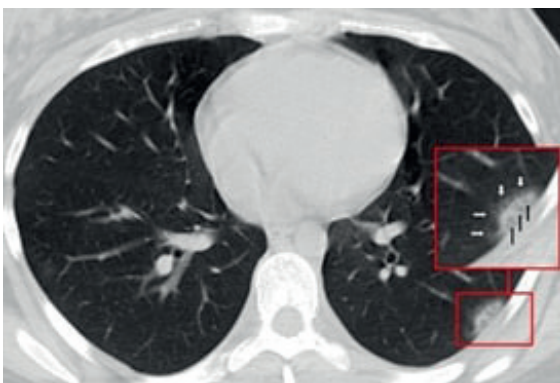


**Fig. 7.** An air bubble sign (black arrows) within a peripheral round consolidation surrounding by a halo sign (white arrows) in the left lower lobe in a 10 year old female.

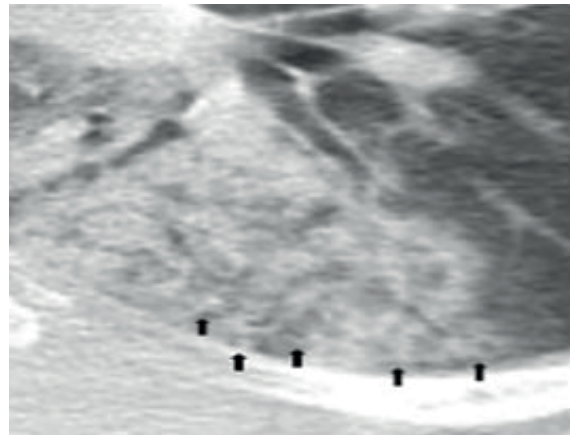


**Fig. 9.** Interlobular septal thickening (black arrows) within a consolidation (crazy paving) in the left lower lobe in a 16 year old male.



**Fig. 10.** Tree-in-bud appearance in right lower lobe in 7 year old male.



**Fig. 13.** A round consolidation (black arrows) in left lower and linear atelectasis (white arrows) in the right lower lobe in a 12 year old male.

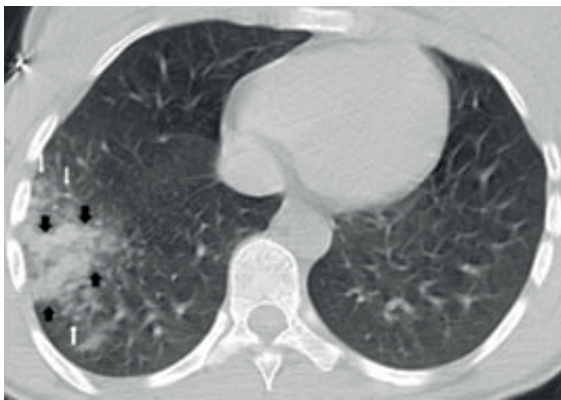


**Fig. 11.** An irregular consolidation (black arrows) and tree-in-bud appearance (white arrows) in a 3 year old male.

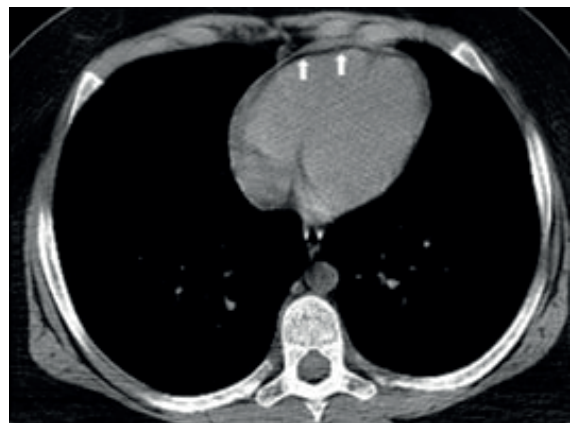


**Fig. 14.** A thin pericardial effusion (white arrows) in a 12 year old male.

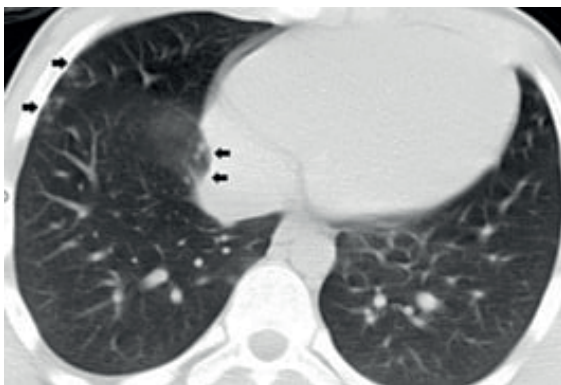


**Fig. 12.** Subpleural nodules (black arrows) in right lower lobe in a 17 year old male.

as normal in 38 of these 42 patients. Focal radiopacities compatible with consolidation were observed in 4 patients (Fig. 18). As a result, focal consolidation was the only pathological finding detected on X-ray of the patients. No other pathological signs were detected on chest X-rays. Pathological findings were also seen on CT scans in all these 4 patients while there was no patient with signs on X-ray who did not have a pathological finding on CT.

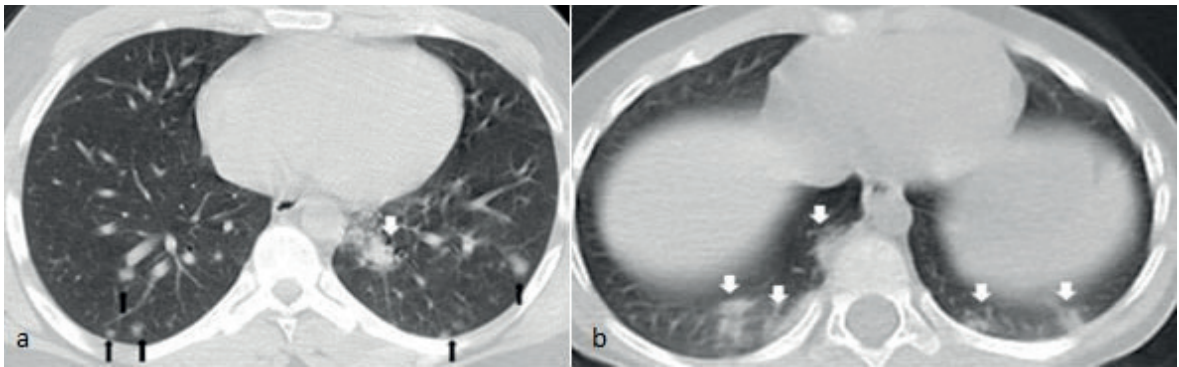


**Fig. 15a-b.** Ground-glass opacities (black arrows) in both lower lobes and consolidation (white arrow) in left lower lobe in a 17 year old male (a). Consolidations (white arrows) in both lower lobes in a 3 year old male (b).

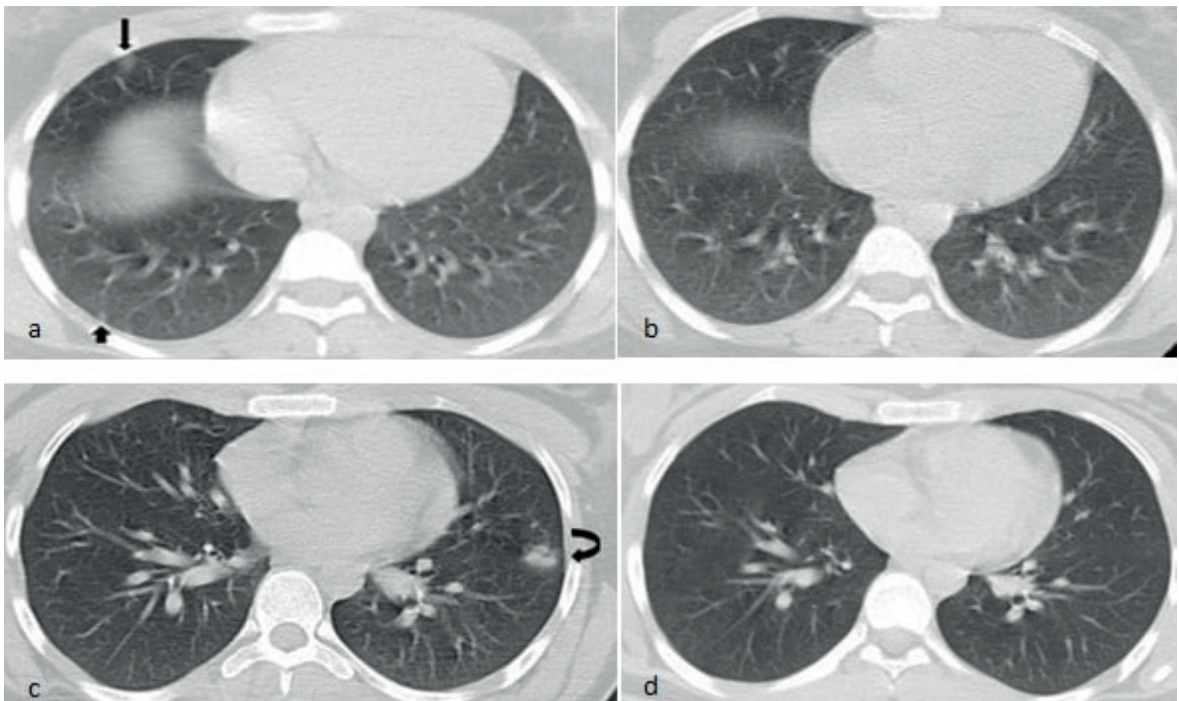


**Fig. 16a-d.** Ground-glass opacities (long black arrow) and a nodule (short black arrow) in a 16 year old male on initial scan (a). Lesions were not seen 7 days after first scan (b). A round consolidation (curved black arrow) in a 8 year old on first scan (c). Lesion disappeared after 7 days (d).

**Discussion**

COVID-19 disease can cause a highly contagious acute infectious pneumonia caused by SARS-CoV-2 that can be transmitted by an infected patient or an asymptomatic carrier. Since most pediatric patients are asymptomatic, they have a critical role in the spread of the disease. In pediatric cases with mild clinical symptoms, usually, a plain chest X-ray does not

provide sufficient information, which leads to misdiagnosis. In some children with negative COVID-19 RT-PCR tests and clinical findings, especially in the initial stages of the disease, a thorax CT examination may be very useful for the diagnosis.<sup>7</sup>

When compared with adult COVID-19 patients, unilateral involvement is higher in pediatric patients.<sup>7,8</sup> Involvement rates of the



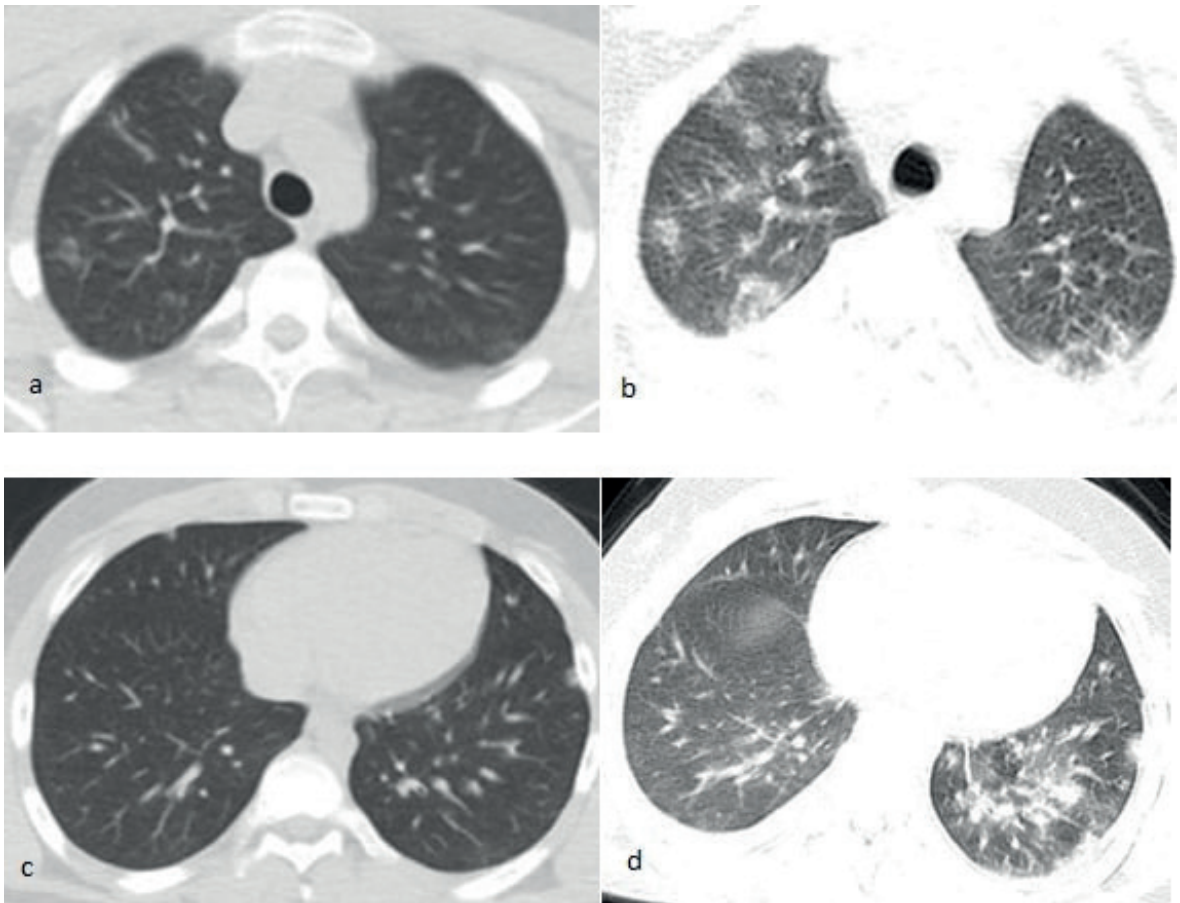


**Fig. 17a-d.** Lesions on first scan of 16 year old male (a-c). Progression of the lesions on the second scan after 15 days (b-d).

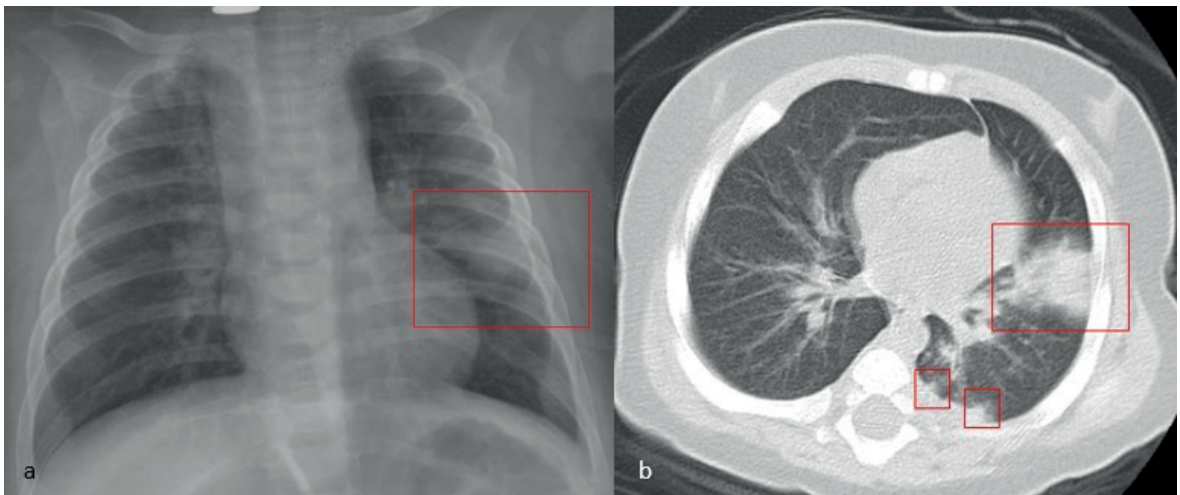


**Fig. 18a-b.** Radiopacity at middle left lung zone on prior X-ray (a) and consistent consolidations on CT (b) of a 5 year old male.

lower lobes are high in pediatric cases.<sup>8,9</sup> In our study, consistent with the literature, lower lobe dominance was present while left lower lobe involvement was the most common. Chen et al.<sup>10</sup> stated that pediatric patients tended to have less extensive involvement than adult patients in their study. Sharon et al.<sup>11</sup> suggested that lesions in pediatric patients predominantly involved 1 or 2 lobes. In a study by Palabiyik et al.<sup>4</sup> single lobe involvement was dominant in pediatric patients as well as unilateral lung involvement. Similar to our data, the number of patients with multiple lesions was found to be higher than with a single lesion.<sup>12</sup> However, our relatively high rate of single lesions may be due to less severity of the involvement or to the early phase of the disease at the time of the CT scan. While parenchymal lung lesions are often located peripherally, both peripheral and central lesions may be seen in the same patient. However, only central involvement is very rare<sup>13,14</sup> as in our study.

In a meta-analysis by Katal et al.<sup>1</sup> isolated ground-glass opacity, consolidation, and the concomitance of ground-glass opacity with consolidation were suggested as the most common findings in children with COVID-19. The most common radiological finding detected in COVID-19 pneumonia is ground-glass opacity. In our study, consistent with the literature, ground-glass opacities were smaller in size with a lower density and they were less diffuse in pediatric patients when compared to adults. Also, interlobular septal thickening less frequently accompanies ground-glass opacities in children.<sup>15,16</sup> Consolidation is common in COVID-19 pneumonia as it can be seen as an isolated finding but concurrence of consolidation and ground-glass opacity may be seen frequently. They become prominent in the peak period of the disease, especially in the posterior and peripheral aspects of the lower lobes. It can be morphologically round, linear, and irregular in shape, and may be accompanied by air bronchograms.<sup>6,7,17,18</sup> In our study, round-shaped consolidation areas

were predominant while linear and irregular consolidations frequently accompanied round consolidations.

Halo sign is termed as the presence of a surrounding ground-glass opacity around a nodule or mass.<sup>19</sup> The halo sign is more common in pediatric COVID-19 cases compared to adult patients.<sup>20</sup> In a study by Xia et al.<sup>7</sup> they stated that the halo sign surrounding the consolidations was observed at a rate of 50% and this finding could be considered specific for pediatric patients. In our study, the frequency of halo sign associated with consolidation areas and nodules was found as 9%. Interlobular septal thickening refers to the collection of inflammatory cells in the interstitium. In COVID-19 pneumonia, it can be isolated or accompanied by ground-glass opacities and consolidation areas ("crazy paving"). This is one of the common findings of COVID-19 pneumonia in adults and it was less frequent in children in our study when compared with studies on adults in the literature.<sup>21-23</sup> Reversed halo sign is one of the atypical findings of COVID-19 pneumonia and is rare in children.<sup>11</sup> Bronchial wall thickening due to airway changes is a finding reflecting the severity of the disease.<sup>24</sup> In a study with 10 pediatric COVID-19 cases, Tan et al.<sup>25</sup> found bronchial wall thickening in 1 patient.

Bronchiectasis may occur due to volume loss during the organization of consolidation areas.<sup>17</sup> The air bubble sign can refer to the pathological expansion of physiological air space in the parenchyma of the lung or the rounded appearance of existing bronchiectasis or the air gaps formed during the resorption of the collapsed structures.<sup>26</sup>

Vascular enlargement is described as an increase in the size of subsegmental pulmonary vessels (> 3 mm), especially in lung areas where parenchymal involvement is more prominent. In patients with COVID-19 pneumonia, these findings may be related to the damage and thickening of the vascular wall structures caused by inflammatory processes.<sup>27</sup> We could

not find detailed data on bronchiectasis, air bubbles, and vascular enlargement in pediatric COVID-19 patients. In our study, we detected bronchiectases in 2 (6%), air bubble finding in one (3%), and vascular enlargement in 2 (6%) patients.

Nodules are round or irregular opacities less than 3 cm in diameter, well or poorly circumscribed, and are often associated with viral pneumonia. Its' incidence in children with COVID-19, is slightly higher than in adult patients.<sup>7,19,28</sup> In our study, 9 (26%) patients had mostly well-circumscribed subpleural and perivascular nodules with a mean diameter of  $4.6 \text{ mm} \pm 1.3$  (3-7 mm). The tree-in-bud finding, which is usually an indicator of small airway disease, is one of the atypical findings of COVID-19. These lesions should raise a suspicion of the presence of bacterial or viral co-infection and patients should be evaluated in this respect.<sup>26</sup> In the study of Xia et al.<sup>7</sup> they concluded that co-infection is seen frequently in pediatric COVID-19 patients (40%). In our study, 3 (9%) patients had nodular infiltration areas. However, we did not have additional sufficient evidence to support the presence of co-infection in these patients.

The incidence of pericardial effusion of adult COVID-19 cases on CT images is approximately 5%<sup>20,29</sup>, but we could not find data about the frequency in pediatric COVID-19 cases. In our study, one patient had pericardial fluid. Pleural fluid and lymphadenopathy in pediatric COVID-19 patients were rarely reported in previous studies.<sup>30</sup> Also, pleural fluid and lymphadenopathy were not found in our study.

The clinicians and radiologists should be in consensus on the evaluation of pediatric patients regarding the sensitivity and specificity of CT, the accuracy of RT-PCR tests, and radiation exposure. It should be kept in mind that CT findings in COVID-19 are not specific and may occur in various diseases such as other viral or atypical pneumonia, hypersensitivity pneumonia, eosinophilic

lung diseases. Also, a relatively lower positive predictive value is another potential limitation of CT especially in some regions with a low COVID-19 prevalence.<sup>5,31</sup> In the new guidelines by the North American Radiology Association (RSNA), the RT-PCR test is suggested as the first method to be used for the diagnosis of COVID-19 in children. They noted that imaging is not indicated unless the patient has potential risk factors or a progression in clinical symptoms.<sup>32</sup>

In the study by Ma et al.<sup>23</sup> they stated that a significant improvement of the lesions was observed in most of the pediatric cases on follow-up images. Therefore, control CT scans should be obtained when they are only necessary, considering the clinical changes in the patients. A guideline by the North American Radiology Association (RSNA)<sup>32</sup>, recommends bidirectional (posterior-anterior and lateral) chest radiography for follow-up pediatric patients with COVID-19.

The primary limitations of the study are its retrospective nature and the relatively small patient number. Also, we could not exclude the presence of a bacterial or viral co-infection in some patients with suspicious CT findings such as nodular infiltrations.

In conclusion the number of pediatric COVID-19 cases is gradually increasing. There are some differences in the thoracic CT features of COVID-19 in children compared to adults. Awareness of CT findings of COVID-19 in children is important for both rapid isolation and control of the disease. The use of CT for the follow-up the pediatric COVID-19 patients must be limited because of the high radiation dose.

### Ethical approval

This study was approved by Kırşehir Ahi Evran University Ethics Committee on 09/02/2021 with the number of 2021-03 / 28.

### Author contribution

The authors confirm contribution to the paper as follows: study conception and design: YD, SÖ; data collection: YD, SÖ, EÜ, RA, MA; analysis and interpretation of results: YD, SÖ, EÜ; draft manuscript preparation: YD, SÖ. All authors reviewed the results and approved the final version of the manuscript.

### Source of funding

The authors declare the study received no funding.

### Conflict of interest

The authors declare that there is no conflict of interest.

### REFERENCES

- Katal S, Johnston SK, Johnston JH, Gholamrezanezhad A. Imaging findings of SARS-CoV-2 infection in pediatrics: a systematic review of Coronavirus Disease 2019 (COVID-19) in 850 patients. *Acad Radiol* 2020; 27: 1608-1621. <https://doi.org/10.1016/j.acra.2020.07.031>
- Dong Y, Mo X, Hu Y, et al. Epidemiology of COVID-19 among children in China. *Pediatrics* 2020; 145: e20200702. <https://doi.org/10.1542/peds.2020-0702>
- Ai T, Yang Z, Hou H, et al. Correlation of chest CT and RT-PCR testing for Coronavirus Disease 2019 (COVID-19) in China: a report of 1014 cases. *Radiology* 2020; 296: E32-E40. <https://doi.org/10.1148/radiol.2020200642>
- Palabiyik F, Kokurcan SO, Hatipoglu N, Cebeci SO, Inci E. Imaging of COVID-19 pneumonia in children. *Br J Radiol* 2020; 93: 20200647. <https://doi.org/10.1259/bjr.20200647>
- Alpaslan M, Özkaçmaz S, Dadalı Y, Dündar İ. COVID-19 tanılı hastalarımızın bilgisayarlı tomografi sonuçları: tipik ve atipik bulgular. *Ahi Evran Med J* 2020; 4: 109-116. <https://doi.org/10.46332/aemj.792717>
- Revel MP, Parkar AP, Prosch H, et al. COVID-19 patients and the radiology department - advice from the European Society of Radiology (ESR) and the European Society of Thoracic Imaging (ESTI). *Eur Radiol* 2020; 30: 4903-4909. <https://doi.org/10.1007/s00330-020-06865-y>
- Xia W, Shao J, Guo Y, Peng X, Li Z, Hu D. Clinical and CT features in pediatric patients with COVID-19 infection: different points from adults. *Pediatr Pulmonol* 2020; 55: 1169-1174. <https://doi.org/10.1002/ppul.24718>
- Chen C, Cao M, Peng L, et al. Coronavirus Disease-19 among children outside Wuhan, China. *Social Science Research Network*. <https://doi.org/10.2139/ssrn.3546071>
- Yu H, Cai Q, Dai X, Liu X, Sun H. The clinical and epidemiological features and hints of 82 confirmed COVID-19 pediatric cases aged 0-16 in Wuhan, China. *medRxiv*. Preprint posted online March 18, 2020. <https://doi.org/10.1101/2020.03.15.20036319>
- Chen A, Huang JX, Liao Y, et al. Differences in clinical and imaging presentation of pediatric patients with COVID-19 in comparison with adults. *Radiol Cardiothorac Imaging* 2020; 2: e200117. <https://doi.org/10.1148/ryct.2020200117>
- Steinberger S, Lin B, Bernheim A, et al. CT features of Coronavirus Disease (COVID-19) in 30 pediatric patients. *AJR Am J Roentgenol* 2020; 215: 1303-1311. <https://doi.org/10.2214/AJR.20.23145>
- Shelmerdine SC, Lovrenski J, Caro-Domínguez P, Toso S; Collaborators of the European Society of Paediatric Radiology Cardiothoracic Imaging Taskforce. Coronavirus disease 2019 (COVID-19) in children: a systematic review of imaging findings. *Pediatr Radiol* 2020; 50: 1217-1230. <https://doi.org/10.1007/s00247-020-04726-w>
- Li B, Shen J, Li L, Yu C. Radiographic and clinical features of children with Coronavirus Disease (COVID-19) pneumonia. *Indian Pediatr* 2020; 57: 423-426. <https://doi.org/10.1007/s13312-020-1816-8>
- Tang A, Xu W, Shen M, et al. A retrospective study of the clinical characteristics of COVID-19 infection in 26 children. *medRxiv*. Preprint posted online March 10, 2020. <https://doi.org/10.1101/2020.03.08.20029710>
- Duan YN, Zhu YQ, Tang LL, Qin J. CT features of novel coronavirus pneumonia (COVID-19) in children. *Eur Radiol* 2020; 30: 4427-4433. <https://doi.org/10.1007/s00330-020-06860-3>

16. Feng K, Yun YX, Wang XF, et al. Analysis of CT features of 15 Children with 2019 novel coronavirus infection. *Zhonghua Er Ke Za Zhi* 2020; 58: E007. <https://doi.org/10.3760/cma.j.issn.0578-1310.2020.0007>
17. Nagpal P, Narayanasamy S, Vidholia A, et al. Imaging of COVID-19 pneumonia: patterns, pathogenesis, and advances. *Br J Radiol* 2020; 93: 20200538. <https://doi.org/10.1259/bjr.20200538>
18. Li W, Cui H, Li K, Fang Y, Li S. Chest computed tomography in children with COVID-19 respiratory infection. *Pediatr Radiol* 2020; 50: 796-799. <https://doi.org/10.1007/s00247-020-04656-7>
19. Hansell DM, Bankier AA, MacMahon H, McLoud TC, Müller NL, Remy J. Fleischner Society: glossary of terms for thoracic imaging. *Radiology* 2008; 246: 697-722. <https://doi.org/10.1148/radiol.2462070712>
20. Bao C, Liu X, Zhang H, Li Y, Liu J. Coronavirus Disease 2019 (COVID-19) CT findings: a systematic review and meta-analysis. *J Am Coll Radiol* 2020; 17: 701-709. <https://doi.org/10.1016/j.jacr.2020.03.006>
21. Shi H, Han X, Jiang N, et al. Radiological findings from 81 patients with COVID-19 pneumonia in Wuhan, China: a descriptive study. *Lancet Infect Dis* 2020; 20: 425-434. [https://doi.org/10.1016/S1473-3099\(20\)30086-4](https://doi.org/10.1016/S1473-3099(20)30086-4)
22. Lu X, Zhang L, Du H; Chinese Pediatric Novel Coronavirus Study Team. SARS-CoV-2 infection in children. *N Engl J Med* 2020; 382: 1663-1665. <https://doi.org/10.1056/NEJMc2005073>
23. Ma H, Hu J, Tian J, et al. Visualizing the novel coronavirus (COVID-19) in children: what we learn from patients at Wuhan Children's Hospital. *Social Science Research Network*. <https://doi.org/10.2139/ssrn.3550012>
24. Li K, Wu J, Wu F, et al. The clinical and chest CT features associated with severe and critical COVID-19 pneumonia. *Invest Radiol* 2020; 55: 327-331. <https://doi.org/10.1097/RLI.0000000000000672>
25. Tan YP, Tan BY, Pan J, Wu J, Zeng SZ, Wei HY. Epidemiologic and clinical characteristics of 10 children with coronavirus disease 2019 in Changsha, China. *J Clin Virol* 2020; 127: 104353. <https://doi.org/10.1016/j.jcv.2020.104353>
26. Ye Z, Zhang Y, Wang Y, Huang Z, Song B. Chest CT manifestations of new coronavirus disease 2019 (COVID-19): a pictorial review. *Eur Radiol* 2020; 30: 4381-4389. <https://doi.org/10.1007/s00330-020-06801-0>
27. Caruso D, Polidori T, Guido G, et al. Typical and atypical COVID-19 computed tomography findings. *World J Clin Cases* 2020; 8: 3177-3187. <https://doi.org/10.12998/wjcc.v8.i15.3177>
28. Azadbakht J, Haghi-Aminjan H, Farhood B. Chest CT findings of COVID-19-infected patients, are there differences between pediatric and adult patients? A systematic review. *Egypt J Radiol Nucl Med* 2020; 51: 145. <https://doi.org/10.1186/s43055-020-00261-8>
29. Wu J, Wu X, Zeng W, et al. Chest CT findings in patients with Coronavirus Disease 2019 and its relationship with clinical features. *Invest Radiol* 2020; 55: 257-261. <https://doi.org/10.1097/RLI.0000000000000670>
30. Zang ST, Han X, Cui Q, Chang Q, Wu QJ, Zhao YH. Imaging characteristics of coronavirus disease 2019 (COVID-19) in pediatric cases: a systematic review and meta-analysis. *Transl Pediatr* 2021; 10: 1-16. 288. <https://doi.org/10.21037/tp-20-281>
31. Kim H, Hong H, Yoon SH. Diagnostic performance of CT and reverse transcriptase polymerase chain reaction for Coronavirus Disease 2019: a meta-analysis. *Radiology* 2020; 296: E145-E155. <https://doi.org/10.1148/radiol.2020201343>
32. Foust AM, Phillips GS, Chu WC, et al. International expert consensus statement on chest imaging in pediatric COVID-19 patient management: imaging findings, imaging study reporting, and imaging study recommendations. *Radiol Cardiothorac Imaging* 2020; 2: e200214. <https://doi.org/10.1148/ryct.2020200214>